Hindawi
Complexity
Volume 2023, Article ID 8260317, 23 pages
https://doi.org/10.1155/2023/8260317

Research Article

A New Bayesian Network-Based Generalized Weighting Scheme for the Amalgamation of Multiple Drought Indices

Muhammad Ahmad Raza,[1,2] **Mohammed M. A. Almazah**,[3] **Nadhir Al-ansari**,[4] **Ijaz Hussain**,[1] **Fuad S. Al-Duais**,[5,6] **and Mohammed A. Naser**[3]

[1]*Department of Statistics, Quaid-i-Azam University, Islamabad, Pakistan*
[2]*Federal Urdu University, Arts, Sciences and Technology, Islamabad, Pakistan*
[3]*Department of Mathematics, College of Sciences and Arts (Muhyil), King Khalid University, Muhyil 61421, Saudi Arabia*
[4]*Department of Civil, Environmental and Natural Resources Engineering, Lulea University of Technology, 971 87 Lulea, Sweden*
[5]*Mathematics Department, College of Humanities and Science, Prince Sattam Bin Abdulaziz University, Al Aflaj, Saudi Arabia*
[6]*Administration Department, Administrative Science College, Thamar University, Thamar, Yemen*

Correspondence should be addressed to Nadhir Al-ansari; nadhir.alansari@ltu.se and Ijaz Hussain; ijaz@qau.edu.pk

Received 2 March 2022; Revised 10 December 2022; Accepted 4 April 2023; Published 21 April 2023

Academic Editor: Ning Cai

Drought is one of the most multifaceted hydrologic phenomena, affecting several factors such as soil moisture, surface runoff, and significant water shortages. Therefore, monitoring and assessing drought occurrences based on a single drought index are inadequate. The current study develops a multiscalar weighted amalgamated drought index (MWADI) to amalgamate multiple drought indices. The MWADI is mainly based on the normalized average dependence posterior probabilities (ADPPs). These ADPPs are obtained from Bayesian networks (BNs)-based Markov Chain Monte Carlo (MCMC) simulations. Results have shown that the MWADI correlates more with the standardized precipitation index (SPI) and the standardized precipitation temperature index (SPTI). As proposed, the MWADI synthesizes drought characteristics of different multiscalar drought indices to reduce the uncertainty of individual drought indices and provide a comprehensive drought assessment.

1. Introduction

Drought has complex nature and slow onset characteristics that have severe impacts on several sectors worldwide [1]. The vulnerabilities of drought differ from other natural hazards in numerous ways [2]. The abrupt and enigmatic features of drought make it the costliest and least understood hazard [3]. The American Meteorological Association classified drought into four categories including meteorological, hydrological, agricultural, and socioeconomic [4, 5]. Each drought category has different causes and consequences [6, 7]. For instance, meteorological drought occurs due to a lack of precipitation. It significantly impacts various sectors such as ecology, agricultural productions, and industrial productions [8]. It causes serious environmental and socioeconomic issues at regional and global scales [9, 10]. Meteorological drought can trigger linked climatic hazards such as pollution and heatwave [11]. Precise drought monitoring of drought requires reliable information, assessment, and evidence-based decisions [12]. Moreover, drought indices play a vibrant role in risk assessment for accurately identifying drought occurrence, severity, and spatial extent [13].

Drought indices are essential for quantifying drought duration, severity, and spatial extent [14, 15]. Various drought indices based on single and multiple climatic parameters have been developed to monitor and assess the drought characteristics [16]. The widely used drought indices are the Palmer drought severity index (PDSI) [17], the surface water supply index (SWSI) [8, 18], the standardized

precipitation index (SPI) [19], the effective drought index (EDI) [20], the standardized precipitation and evapotranspiration index (SPEI) [21], and the standardized precipitation temperature index (SPTI) [22]. Moreover, the SPI is the most well-known drought index proposed by the World Meteorological Organization (WMO). However, the selection and calculation of drought indices depend on the availability of data-related input climatic indicators [23]. Furthermore, due to the complex nature of hydroclimatic parameters, traditional meteorological drought indices cannot obtain full information for accurate drought characterization [24].

Individual drought indices have certain deficiencies in assessing drought severities [25]. The substantial complexity of the hydrological process depends upon multiple climatic factors such as precipitation, temperature, and evapotranspiration [26]. Single drought indices are incapable of considering certain drought-induced causes, leading to inaccurate drought assessment [27]. However, a very few composite and hybrid drought indices have been observed in recent decades [28]. The vegetation drought response index (VegDRI) is one of the best examples of a comprehensive drought index based on the SPI, the PDSI, and the NDVI [29]. Numerous drought indices are constructed using linear combinations, principal component analysis, and entropy weight method by considering a linear relationship among standardized drought indices [30]. However, regardless of the type of drought, the interactions among the numerous influencing factors in the environment should be considered for drought monitoring. Generally, drought conditions are associated with multiple meteorological and climatic variables [31]. Therefore, a comprehensive drought index based on a strong probabilistic structure can provide more accurate information about drought monitoring and assessing drought conditions.

Bayesian networks (BNs) are powerful probabilistic graphical models that explicitly capture the known dependence structure among stochastic variables such as drought indices (DIs) with probabilities through directed acyclic graphs (DAGs) [32]. The BNs have wide applications in various fields, viz., computer science [33], business analytics [34], agriculture [35], genetics [36], and environmental sciences [37, 38]. BNs are appropriate methods to estimate climate change impact and drought risk assessment [39]. The researchers have used the BN algorithm to develop new frameworks in different fields. For instance, it is used for flood prediction [40] and forecasting the dependence structure among health outcomes and hazardous pollutants [41]. Shin et al. (2020) used BNs to propagate the relationships of hydrological drought in different time intervals. Ávila and Ballari [42] used BNs to develop new homogeneous climate zone indices. Appraisal of the latest literature indicated that BNs are emerging in meteorological and climatic studies. The potential of probabilistic graphical models based on BNs for drought assessment and developing new comprehensive drought indices could be helpful. Since droughts are a slowly evolving phenomenon, a robust spatial and temporal relationship exists among drought indices [43]. Therefore, they can be amalgamated using BNs to combine the strengths of several drought indices.

The current study aims to develop a comprehensive drought index to improve the monitoring and assessment of drought. For this purpose, the current research uses the BN theory to synthesize drought monitoring characteristics of three standardized drought indices, including the SPI, the SPEI, and the SPTI. The proposed framework based on the Bayesian network theory also integrates the seasonal component of several seasonally segregated drought indices. It provides a scientific basis for an effective drought mitigation plan [44]. Moreover, the Gilgit-Baltistan province is selected to validate the current research.

2. Materials and Methods

2.1. Data Description and Study Area. The six synoptic gauged meteorological stations have been selected, including Astore, Bunji, Chilas, Gilgit, Gupis, and Skardu. The monthly time series data of precipitation and temperature (maximum and minimum) have been used to develop the MWADI. The input data for 47 years ranging from 1970 to 2016 have been acquired from the Karachi Data Processing Center (KDPC) through the Pakistan Meteorological Department (PMD). The spatial distribution map and location information of selected meteorological stations of Gilgit-Baltistan province is shown in Figure 1. The study area lies between 34.5125°N–37.0826°N latitude and 72.508°E–77.01°E longitude. The terrain feature of the study area is high-elevation mountainous. The GB province comprises the upper catchment areas of the Indus River and its major tributaries. The source of precipitation in GB is the typical continental monsoon in summer and the western depression in winter. The average annual rainfall in GB province is 231.5 inches. However, the region's temporal and spatial distributions of precipitation are not homogenous. The mean average annual precipitation at these selected meteorological stations significantly varies, as shown in Table 1. According to the above characteristics of topography, hydrology, and geomorphology, the region's climate is classified into different categories. The climate classification of selected meteorological stations is given in the last column of Table 1. These climate classifications are known as Köppen climate classifications [45]. Köppen [46] classified the climate of any region into five categories, which were further divided into subcategories. According to Köppen classification, the climate of Astore is considered humid-continental, and Gilgit and Bunji are considered cold desert, while Chilas, Gupis, and Skardu are classified as cold semiarid. The descriptive statistics of spatial variables (longitude, latitude, and elevation) and meteorological variables (precipitation and minimum and maximum temperature) are given in Table 1. It includes the mean and standard deviation (SD) of the average annual precipitation of selected meteorological stations. It provides varying features of the minimum and maximum temperature.

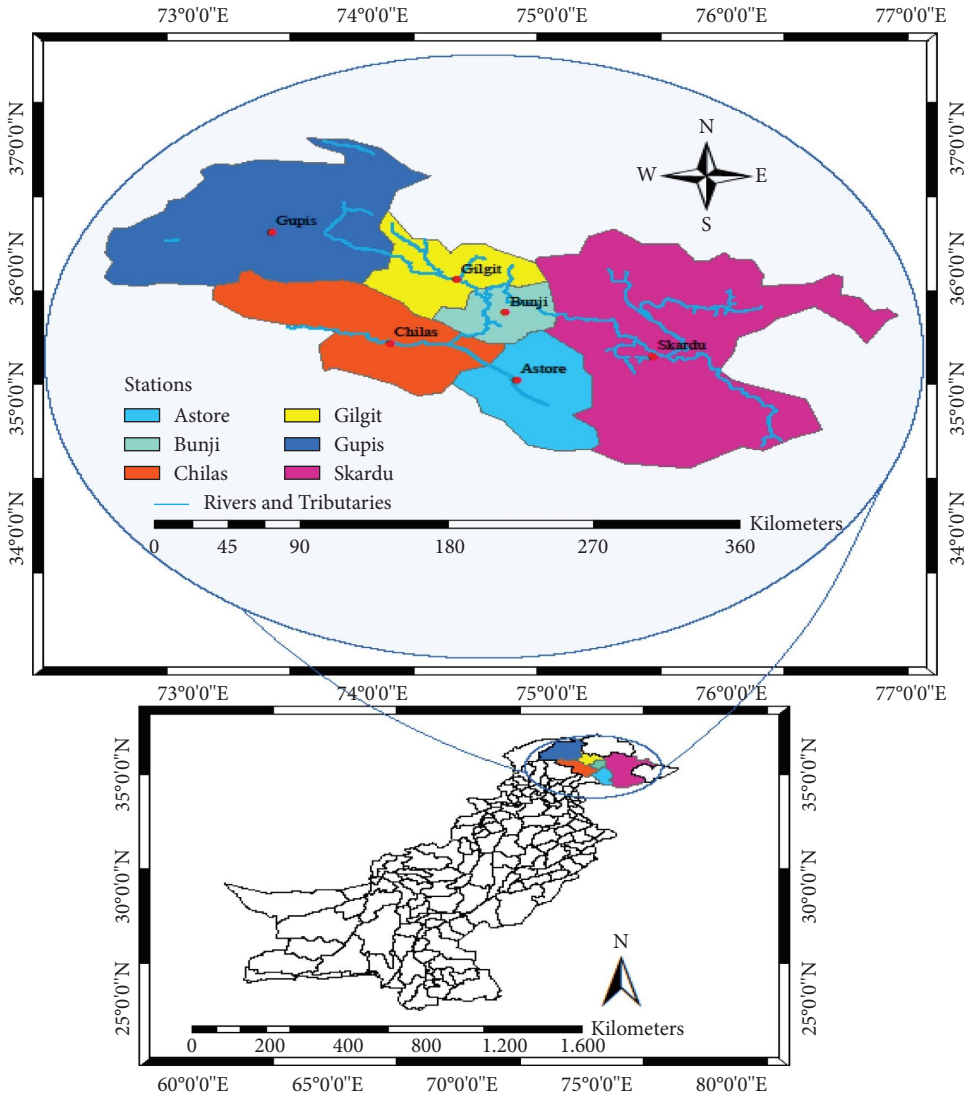

Figure 1: The map of the study region and distribution of meteorological stations.

Table 1: Descriptive statistics of average annual meteorological variables (precipitation and minimum and maximum temperature), regional spatial characteristics, and climate (Köppen classification).

Station	Precipitation		Temp. min		Temp. max		Latitude	Longitude	Elevation (m)	Climate
	Mean	SD	Min	Max	Min	Max				
Astore	471.8	129.3	2.36	5.23	13.90	17.47	35.3570°E	74.8624°N	2546	Humid continental
Bunji	163.4	61.5	9.57	13.6	22.33	25.48	35.6431°E	74.6342°N	1453	Cold desert
Chilas	190.6	93.9	12.32	15.53	24.57	27.97	35.4222°E	74.0946°N	1265	Cold semiarid
Gilgit	140.7	49.4	6.15	9.26	22.45	25.92	35.8819°E	74.4643°N	1500	Cold desert
Gupis	190.4	145.2	4.19	8.33	16.99	20.54	36.2274°E	73.4421°N	3030	Cold semiarid
Skardu	231.9	95.5	3.31	6.17	16.29	20.81	35.3247°E	75.551°N	2228	Cold semiarid

2.2. A Brief Description of Multiscalar Standardized Drought Indices. Standardized drought indices (SDIs) play a vibrant role in drought risk assessment and the sustainable development of water resources [9]. Therefore, defining drought features specific to drought intensity, duration, and patterns is very important [21]. Thus, the multiscaler drought indices, such as the SPI, the SPEI, and the SPTI, are selected as input hydroclimatic variables to develop the MWADI. The standardized precipitation index (SPI) is the most widely used drought index applied to regional and global studies. The World Meteorological Organization (WMO) ratified the SPI for meteorological drought [47]. It is a probabilistic and spatially invariant indicator for a different type of drought analysis [48]. The SPI utilizes only precipitation and has the inherited capability to be calculated at various time scales [49]. The standardized precipitation evapotranspiration

index (SPEI) is a climatic water balance variant of the SPI based on precipitation and potential evapotranspiration. It possesses the multiscalar capability of the SPI by considering its simple mathematical procedure and utilizing temperature variability. The computation procedure of the SPEI is followed by guidelines provided in [50]. The standardized precipitation temperature index (SPTI) is another multiscalar drought selected as the input climatic indicator of our proposed framework. The calculation procedure of the SPTI is quite like the SPI and the SPEI.

The above-stated drought indices are standardized, i.e., cumulative distribution function (CDF) values of a normal probability distribution. For any time scale, the zero value of SDIs (the SPI, the SPEI, and the SPTI) stated that there is no deviation from the average precipitation. A positive value indicates that the precipitation is higher than the average precipitation. In contrast, a negative value of drought shows that precipitation is smaller than the average precipitation.

2.3. Seasonality of Drought Indices. Drought predictions using seasonally integrated drought indices are helpful in freshwater resource management and ecological preservation [51]. Seasonal segregation of drought indices can compute hybrid and comprehensive drought indices for precise drought characterization [52, 53]. The seasonal climate forecast usually ranges from a few weeks to a year but is mainly selected at a monthly scale [54], as various hydrological and climatological studies are based on monthly defined seasonal indices [55, 56]. Similarly, current study indorses monthly defined seasonal drought indices as input variables.

2.4. Bayesian Networks (BNs). Bayesian networks (BNs) are probabilistic graphical models that can describe concise conditional dependence structures among a set of random variates through directed acyclic graphs (DAG) [57]. A DAG consists of nodes representing random variables and arcs or edges that quantify the conditional dependence of random variates (nodes) [39, 58]. The direction of edges or arcs represents the causal relationship among the random variables, and if nodes did not connect through some arc, they are considered conditionally independent. The conditional independence of nodes enables BNs to efficiently represent complex probability distributions [59]. The causal relationship between random variables (nodes) is defined as conditional probability based on prior information or statistically observed correlations [60]. Each node possesses signified states or levels [61]. BNs are constructed for the identification of the dependence structure among random variables. The learning of BNs from data for inference and decision-making is based on Markov Chain Monte Carlo (MCMC) algorithms [62, 63] using an improved Metropolis–Hastings sampler [64, 65].

In the Bayesian network theory, to learn the Bayesian networks from some observed dataset E, the posterior probability of network G can be computed using the Bayes rule.

$$P(G|E) = \frac{P(E|G)P(G)}{P(E)}, \tag{1}$$

where $P(E|G)$ is the marginal likelihood function of observed data given the DAG G', $P(G)$ is the prior density of DAG, and $P(E)$ is the normalizing factor. Then, the posterior probability of any hypothesis of interest can be computed by averaging all networks. For a detailed description of Bayesian learning, the Bayesian model average approach, and marginal posterior of features (edges), see [66].

2.5. Proposed Framework for the Bayesian Network-Based Generalized Weighting Scheme for Amalgamation of Multiple Drought Indices. The main objective of this study is to introduce a Bayesian network-based new weighting scheme for amalgamating multiple seasonal drought indices to develop a new comprehensive drought index. The central part of the study is based on three standardized drought indices (the SPI, the SPEI, and the SPTI) and the Bayesian network procedure. The details of these methodologies have already been discussed in Sections 2.2 and 2.3. A schematic diagram of the proposed framework is shown in Figure 2. Further implication and execution of the framework comprise different phases, which are as follows.

Phase 1. Selection and calculation of SDIs (the SPI, the SPEI, and the SPTI): The selection of drought indices can influence the obtained information about drought monitoring, its areal extent, and duration. Most of the SDIs are region-specific and have inherited complexities. Therefore, single and multiple meteorological variables based on drought indices (the SPI, the SPEI, and the SPTI) have been selected for the current study, and their calculation procedure is briefly described in Section 2.2.

Phase 2. Seasonal segregation of SDIs: In this phase, full-length time series datasets of already calculated SDIs are separated with respect to months by considering each month as a season for seasonal, temporal formation [56, 67]. These seasonal drought indices are then considered as input variables for structural BNs.

Phase 3. The implication of BNs to obtain potion quantities (weights): The key objective of the current study is to estimate the probabilistic dependence structure of seasonal standardized drought indices (the SPI, the SPEI, and the SPTI) at each selected meteorological station. The marginal posterior probabilities of feature edges (nodes/variables) are approximated through Markov Chain Monte Carlo (MCMC) simulations. Three independent MCMC simulations have run on each time series dataset to obtain convergence, and the marginal posterior probabilities are averaged. The marginal posterior probabilities describe the dependence structure among input variables (seasonal SDIs).

Let SDI_j be the list of candidate standardized drought indices and Y_{ijt} be the time series data of i^{th} season (month)

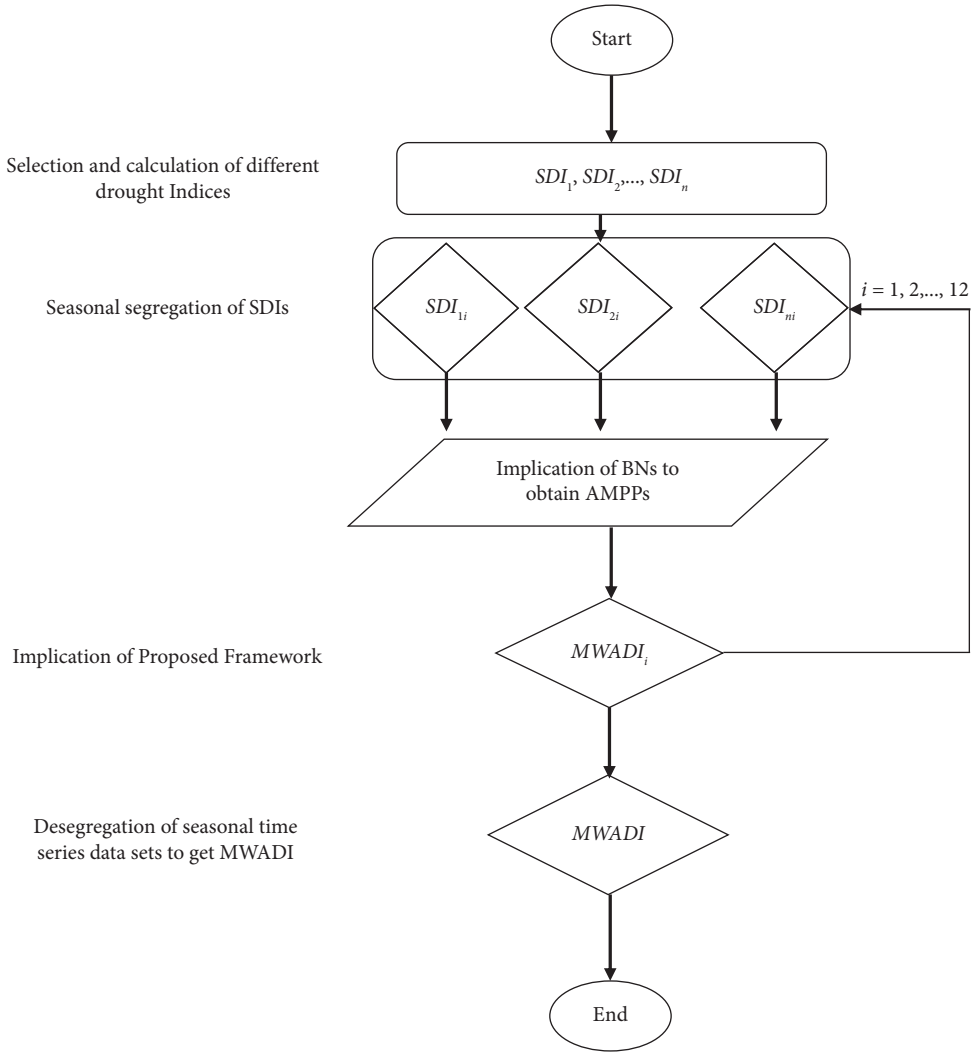

Figure 2: Graphical representation of the proposed framework.

related to j^{th} SDI at any individual meteorological station, where t shows the time index and $(i = 1, 2, \ldots, 12)$, $(j = 1, 2, 3)$. This step aims to calculate potion quantities being used as normalizing weights of the proposed framework to calculate the new seasonally synthesized amalgamated drought index. The realization of nodes (SDI_j) and edges are defined as follows:

$$f\left(y_{i1}, y_{i2}, y_{i3}\right) = P\left(Y_{i1} = y_{i1}, Y_{i2} = y_{i2}, Y_{i3} = y_{i3}\right). \quad (2)$$

Equation (2) describes the relative importance of each seasonal SDI through marginal posterior probabilities, which can also be defined as dependence probability. A single run of MCMC simulation gives the following result:

$$\begin{array}{c} \\ \mathrm{SPI} \\ \mathrm{SPEI} \\ \mathrm{SPTI} \end{array} \begin{array}{c} \begin{array}{ccc} \mathrm{SPI} & \mathrm{SPEI} & \mathrm{SPTI} \end{array} \\ \begin{bmatrix} \pi_{11} & \pi_{12} & \pi_{13} \\ \pi_{21} & \pi_{22} & \pi_{23} \\ \pi_{31} & \pi_{32} & \pi_{33} \end{bmatrix} \end{array}. \quad (3)$$

The average dependence probability (ADP) for a single MCMC simulation of j^{th} seasonal SDI is denoted by $\pi_{.j}$ which is defined as follows:

$$\pi_{.j} = \frac{\pi_{1j} + \pi_{2j} + \pi_{3j}}{3}. \quad (4)$$

The grand average dependence probability (GADP) of j^{th} SDI is denoted by ω_j, finally obtained through averaging for all three MCMC simulations, and is mathematically defined as follows:

$$\omega_j = \frac{\left(\pi_{.j_1} + \pi_{.j_2} + \pi_{.j_3}\right)}{3}. \quad (5)$$

These grand averaged dependence probabilities are the actual probabilistic relative importance of SDIs at each meteorological station. Furthermore, these are considered as potion quantities to calculate normalizing weights ω_j' defined as follows:

$$\omega_j' = \frac{\omega_j}{\sum_{j=1}^{3}\omega_j}, \tag{6}$$

where ω_j' are the estimated parameters of the proposed model defined in equation (6). These parameters are estimated through the probabilistic dependence structure of BNs analytically evaluated through MCMC simulations.

Phase 4. The execution of the proposed model to obtain the seasonal MWADI:

In this phase, a probabilistic model is defined to synthesize information from different SDIs. In numerous studies, stochastic models such as copulas were employed to combine drought characteristics of different drought indices [68–70]. But BNs are structural probabilistic and powerful graphical algorithms to produce dependence probabilities of stochastic variates utilizing every bit of information [40, 63, 71]. Therefore, this study proposes a probabilistic model defined in equation (7), which synthesizes information obtained from seasonal multiscalar standardized drought indices.

$$\mathrm{MWADI}_i = \omega_1'\mathrm{SPI}_i + \omega_2'\mathrm{SPEI}_i + \omega_3'\mathrm{SPTI}_i, \tag{7}$$

where MWADI_i is a linear combination of SPI_i, SPEI_i, and SPTI_i. The linear combination is a mathematical way to combine different drought indices to synthesize the meteorological information related to drought characterization. The most innovative feature of MWADI_i is that the weights (parameters) are calculated through a probabilistic structure of BNs using MCMC simulations. The weights calculated using BNs define the role of different drought indices. The proposed model defined in equation (7) results in seasonal MWADI_i (Jan–Dec) at each station using probabilistic weights or parameters associated with different drought indices. After obtaining the seasonal MWADI_i (Jan–Dec), all 12-time series datasets will be combined to obtain the final MWADI. The outcome of the algorithm is a comprehensive multiscalar weighted amalgamated drought index (MWADI).

3. Results and Discussion

The latest development of drought indices emphasized incorporating complete information readily available in standardized drought indices. Therefore, three multiscalar standardized drought indices (the SPI, the SPEI, and the SPTI) have been used as input indicators to construct the proposed MWADI. The main steps involved in the construction and development of the MWADI are explained and executed in sequence.

3.1. Selection and Estimation of Input Variables (SDIs). The SPI, the SPEI, and the SPTI are estimated using their input meteorological variables for full-length time series data of precipitation and temperature (minimum and maximum) at selected meteorological stations. These drought indices are calculated using a parametric approach by selecting appropriate probability distributions [50]. The Bayesian information criterion (BIC) has been used to determine appropriate distribution using the propagate *R* Package (Spies, 2014). Detailed calculation procedures of these SDIs at these selected meteorological stations can be seen in [66]. Afterward, the datasets of these SDIs are further seasonally (monthly defined) segregated to integrate seasonal components. In this study, six meteorological stations have been selected, and 36 seasonal datasets have formed at each station. Hence, 216 seasonal datasets have been used as input variables to execute MCMC simulations.

3.2. The Implication of BNs for the Estimation of Parameters (Normalizing Weights). The Bayesian network theory has been applied to monthly separated time series data of various drought indices (the SPI, the SPEI, and the SPTI) for calculating their relative importance through the dependence probability structure. BN-based MCMC simulations were performed using seasonal SDIs at each selected meteorological station. BNs sorted out causal relationships between nodes (variable) through DAGs. In this study, seasonal SDIs are considered as nodes, and the arc's direction shows the hydrologic causality (conditional dependence) between nodes (SDIs). Three independent MCMC simulation runs are carried out on monthly separated time series datasets of the SPI, the SPEI, and the SPTI with 200,000 iterations to obtain experimental results. The marginal posterior probabilities or dependence probabilities for each simulation run are obtained using equation (2) for all 12 seasons (Jan–Dec) at each station. The average dependence probabilities (ADPs) are calculated using equation (4). Moreover, ADPs obtained through these independent simulation runs have not shown much variation, which shows the consistency and convergence of MCMC simulation runs. For more precise results, equation (5) calculates grand averaged dependence probabilities (GADPs) by averaging ADPs for all three simulation runs. Tables 2 and 3comprise average marginal posterior probabilities already named ADPs of three simulation runs and GADPs for January and February seasons at all meteorological stations. These GADPs show the relative importance of seasonal SDIs (the SPI, the SPEI, and the SPTI) over each other. The GADPs of the SPI, the SPEI, and the SPTI for January are 0.9907, 0.6528, and 0.6620, respectively, showing the SPI's dominance at the Astore station. While at Bunji station, these results are 0.7245, 0.6429, and 0.9184, respectively. Here, the SPTI dominates other indices, showing that the relative importance of SDIs substantially varies from station to station.

Furthermore, we have checked across seasonal probabilistic relative importance of SDIs (the SPI, the SPEI, and the SPTI). The GADPs for the February season at Astore station are 0.9814, 0.6643, and 0.6829, respectively. The comparison of GADPs across seasons shows that at Astore station, the SPI's dominance persisted. While at Bunji station for the February season, these probabilities are 0.8510, 0.6119, and 0.7608, respectively, depicting that dominance changed from the SPTI to the SPI. The spatial and seasonal variations of conditional relevance of different SDIs are shown in Figure 3. It indicates that SDIs have significant

Table 2: Bayesian network-based grand average dependence probabilities (ω_j) of SDIs for season-1 (January) at all meteorological stations.

Simulation Runs	SDIs	Astore			Bunji			Chilas			Gilgit			Gupis			Skardu		
		SPI	SPEI	SPTI	SPI	SPEI	SPTI	SPI	SPEI	SPTI	SPI	SPEI	SPTI	SPI	SPEI	SPTI	SPI	SPEI	SPTI
	SPI	0.0001	0.9821	1	0.0001	0.4537	1	0.0001	0.4274	1	0.0001	0.4798	1	0.0001	0.4474	1	0.0001	0.8639	1
Run-1	SPEI	0.9821	0.0001	0.3235	0.4537	0.0001	0.8327	0.4274	0.0001	0.8325	0.4798	0.0001	0.7821	0.4474	0.0001	0.8046	0.8639	0.0001	0.3272
	SPTI	1	0.3235	0.0001	1	0.8327	0.0001	1	0.8325	0.0001	1	0.7821	0.0001	1	0.8046	0.0001	1	0.3272	0.0001
ADP_1		0.9910	0.6528	0.6618	0.7268	0.6432	0.9164	0.7137	0.6299	0.9163	0.7399	0.6310	0.8911	0.7237	0.6260	0.9023	0.9320	0.5956	0.6636
	SPI	0.0001	0.9802	1	0.0001	0.4402	1	0.0001	0.4306	1	0.0001	0.4770	1	0.0001	0.4590	1	0.0001	0.7978	1
Run-2	SPEI	0.9802	0.0001	0.3280	0.4402	0.0001	0.8401	0.4306	0.0001	0.8262	0.4770	0.0001	0.7844	0.4590	0.0001	0.7944	0.7978	0.0001	0.4539
	SPTI	1	0.3280	0.0001	1	0.8401	0.0001	1	0.8262	0.0001	1	0.7844	0.0001	1	0.7944	0.0001	1	0.4539	0.0001
ADP_2		0.9901	0.6541	0.6640	0.7201	0.6402	0.9200	0.7153	0.6284	0.9131	0.7385	0.6307	0.8922	0.7295	0.6267	0.8972	0.8989	0.6258	0.7269
	SPI	0.0001	0.9821	1	0.0001	0.4533	1	0.0001	0.4233	1	0.0001	0.4884	0.9998	0.0001	0.4433	1	0	0.8135	1
Run-3	SPEI	0.9821	0.0001	0.3207	0.4533	0.0001	0.8376	0.4233	0.0001	0.8299	0.4886	0.0001	0.7676	0.4433	0.0001	0.8095	0.8135	0.0001	0.4686
	SPTI	1	0.3207	0.0001	1	0.8376	0.0001	1	0.8299	0.0001	1	0.7677	0.0001	1	0.8095	0.0001	1	0.4686	0.0001
ADP_3		0.9910	0.6513	0.6603	0.7266	0.2266	0.9188	0.7117	0.2116	0.9149	0.7443	0.2442	0.8837	0.7216	0.2216	0.9047	0.9068	0.4068	0.7343
GADP		0.9907	0.6528	0.6620	0.7245	0.6429	0.9184	0.7136	0.6283	0.9148	0.7409	0.6299	0.8890	0.7250	0.6263	0.9014	0.9125	0.7083	0.7083

Table 3: Bayesian network-based grand average dependence probabilities (ω_j) of SDIs for February at all stations.

Simulation Runs	SDIs	Astore			Bunji			Chilas			Gilgit			Gupis			Skardu		
		SPI	SPEI	SPTI	SPI	SPEI	SPTI	SPI	SPEI	SPTI	SPI	SPEI	SPTI	SPI	SPEI	SPTI	SPI	SPEI	SPTI
	SPI	0.0001	0.9661	1	0.0001	0.6938	1	0.0001	0.4204	1	0.0001	0.4876	1	0.0001	0.4967	1	0.0001	0.3337	1
Run-1	SPEI	0.9661	0.0001	0.3676	0.6938	0.0001	0.5231	0.4204	0.0001	0.8527	0.4876	0.0001	0.7487	0.4967	0.0001	0.8615	0.3337	0.0001	0.9976
	SPTI	1	0.3676	0.0001	1	0.5231	0.0001	1	0.8527	0.0001	1	0.7487	0.0001	1	0.8615	0.0001	1	0.9976	0.0001
ADP_1		0.9831	0.6669	0.6838	0.8469	0.6084	0.7615	0.7102	0.6366	0.9264	0.7438	0.6181	0.8743	0.7484	0.6791	0.9307	0.6669	0.6656	0.9988
	SPI	0.0001	0.9602	1	0.0001	0.7042	1	0.0001	0.4098	1	0.0001	0.4978	1	0.0001	0.5020	1	0.0001	0.3647	1
Run-2	SPEI	0.9602	0.0001	0.3696	0.7042	0.0001	0.5247	0.4098	0.0001	0.8550	0.4978	0.0001	0.7399	0.5020	0.0001	0.8596	0.3647	0.0001	0.9969
	SPTI	1	0.3696	0.0000	1	0.5247	0.0001	1	0.8550	0.0001	1	0.7399	0.0001	1	0.8596	0.0001	1	0.9969	0.0001
ADP_2		0.9801	0.6649	0.6848	0.8521	0.6144	0.7623	0.7049	0.6324	0.9275	0.7489	0.6188	0.8700	0.7510	0.6808	0.9298	0.6824	0.6808	0.9985
	SPI	0.0001	0.9623	1	0.0001	0.7083	1	0.0001	0.4247	1	0.0001	0.4874	1	0.0001	0.5065	1	0.0001	0.3262	1
Run-3	SPEI	0.9623	0.0001	0.3601	0.7083	0.0001	0.5171	0.4247	0.0001	0.8407	0.4874	0.0001	0.7491	0.5065	0.0001	0.8574	0.3262	0.0001	0.9967
	SPTI	1	0.3601	0.0001	1	0.5171	0.0001	1	0.8407	0.0001	1	0.7491	0.0001	1	0.8574	0.0001	1	0.9967	0.0001
ADP_3		0.9811	0.4811	0.6800	0.8541	0.3541	0.7586	0.7124	0.2124	0.9203	0.7437	0.2437	0.8745	0.7533	0.2533	0.9287	0.6631	0.1631	0.9984
GADP		0.9814	0.6643	0.6829	0.8510	0.6119	0.7608	0.7092	0.6339	0.9247	0.7454	0.6284	0.8729	0.7509	0.6806	0.9298	0.6708	0.6693	0.9985

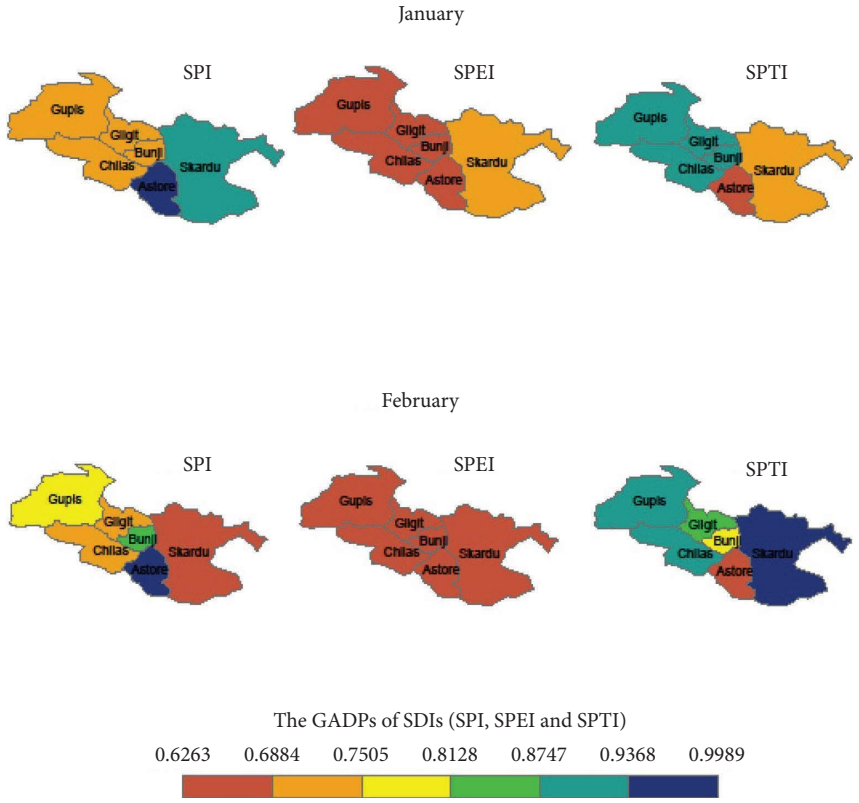

Figure 3: Spatial and seasonal dominance of different SDIs (the SPI, the SPEI, and the SPTI).

seasonal and spatial relevance at some meteorological stations. The GADPs (probabilistic relative importance) of SDIs are further normalized according to equation (6) to obtain the final potion quantities of the algorithm considered as estimates of the parameters of the proposed model. Results for all the 12 seasons (Jan–Dec) and all selected stations are given in Table 4. For ease of understanding, the presentation of experimental results is presented only for the specific season; however, the results for the other seasons can be presented accordingly.

3.3. Execution of the Proposed Model. The proposed model defined in equation (7), the MWADI, is a linear combination of three multiscalar standardized drought indices whose weights (parameters) are calculated using probabilistic structural BNs. The results of these estimated parameters of the proposed model for all the seasons (Jan–Dec) at selected stations are presented in Table 4. The outcome of the proposed model is also the seasonal MWADI for a specific season at each meteorological station. After calculating seasonal MWADIs (Jan–Dec), all 12-time series are then desegregated to obtain an outcome named MWADI. The process is repeated at each meteorological station to obtain the MWADI. The outcome of the proposed algorithm is a seasonally integrated multiscalar amalgamated drought index (MWADI) for any individual meteorological station. The MWADI and input SDIs can be calculated at various temporal scales to monitor drought conditions, but for convenience, results are given for a one-month time scale.

A validation experiment was carried out to assess the accuracy of the drought severity characterized by the MWADI by comparing the count plots, scatter plots, temporal plots, and correlation coefficients. Figures 4–6 show the scatter plots of seasonal MWADI with the SPI, the SPEI, and the SPTI for all seasons Jan–Dec at the Astore station. The MWADI is highly correlated with these drought indices, and the correlation test was applied, and it is observed that the MWADI is significantly correlated with all other SDI's at p value <0.001. Figure 7 shows that the MWADI is slightly less correlated with the SPEI while strongly correlated with the SPI and the SPTI. The overall correlation coefficient values between the MWADI and other SDIs (the SPI, the SPEI, and the SPTI) are 0.93, 0.84, and 0.98, respectively. Results related to the correlation coefficient between the MWADI and other SDIs for all seasons at selected stations are presented in Table 5. The strong relationship between the MWADI and other meteorological SDIs reflects that the MWADI can more precisely monitor and characterize meteorological drought.

The drought occurrence frequency is one of the important factors of drought characterization. Drought severity is classified into seven mutually exclusive categories. Several studies already endorse these classifications [19, 21, 72, 73]. The comparison of different drought categories characterized by the MWADI and other SDIs is presented by count plots, as shown in Figure 8. The frequency of different drought categories significantly varied from one SDI to another and seemed quite uncertain. Because different drought indices give contradictory outcomes

Table 4: Estimated parameters (ω_j') of the proposed model at all meteorological stations for all seasons (Jan–Dec).

Seasons	Astore			Bunji			Chilas			Gilgit			Gupis			Skardu		
	SPI	SPEI	SPTI	SPI	SPEI	SPTI	SPI	SPEI	SPTI	SPI	SPEI	SPTI	SPI	SPEI	SPTI	SPI	SPEI	SPTI
Jan	0.4297	0.2831	0.2872	0.3170	0.2813	0.4018	0.3162	0.2784	0.4054	0.3279	0.2787	0.3934	0.3218	0.2780	0.4001	0.4138	0.2931	0.2931
Feb	0.4215	0.2853	0.2933	0.3827	0.2752	0.3421	0.3127	0.2795	0.4078	0.3333	0.2765	0.3903	0.3180	0.2883	0.3938	0.2868	0.2862	0.4270
Mar	0.3592	0.3198	0.3210	0.3133	0.2803	0.4064	0.3322	0.2880	0.3798	0.3430	0.2769	0.3801	0.3279	0.2779	0.3942	0.2839	0.2834	0.4327
Apr	0.3767	0.3010	0.3223	0.3158	0.2809	0.4033	0.3381	0.2797	0.3822	0.3430	0.2768	0.3801	0.3918	0.2763	0.3318	0.2892	0.2891	0.4217
May	0.3072	0.2957	0.3971	0.2947	0.2867	0.4186	0.2976	0.2850	0.4174	0.2993	0.2862	0.4145	0.2979	0.2847	0.4173	0.2870	0.2870	0.4261
Jun	0.2899	0.2832	0.4268	0.3165	0.2871	0.3964	0.3141	0.2788	0.4072	0.3237	0.2845	0.3918	0.3139	0.2815	0.4046	0.3029	0.2838	0.4133
Jul	0.2853	0.2830	0.4316	0.3038	0.2912	0.4051	0.3117	0.2805	0.4079	0.3117	0.2881	0.4002	0.3144	0.2858	0.3997	0.2972	0.2849	0.4179
Aug	0.2901	0.2856	0.4244	0.2952	0.2882	0.4166	0.3057	0.2810	0.4133	0.2998	0.2830	0.4172	0.3119	0.2804	0.4077	0.2864	0.2847	0.4289
Sep	0.3717	0.2933	0.3350	0.3063	0.2802	0.4135	0.3294	0.2814	0.3891	0.3285	0.2774	0.3941	0.3329	0.2779	0.3892	0.2874	0.2872	0.4254
Oct	0.3556	0.2817	0.3627	0.3711	0.2757	0.3532	0.3367	0.2784	0.3849	0.3845	0.2751	0.3403	0.3727	0.2753	0.3520	0.2840	0.2840	0.4319
Nov	0.3494	0.2815	0.3691	0.3410	0.2744	0.3846	0.3174	0.2827	0.3999	0.3356	0.2759	0.3884	0.3414	0.2750	0.3836	0.2857	0.2840	0.4303
Dec	0.3451	0.2835	0.3714	0.3480	0.2747	0.3773	0.3179	0.2832	0.3988	0.3423	0.2746	0.3832	0.3403	0.2749	0.3848	0.3099	0.3098	0.3803

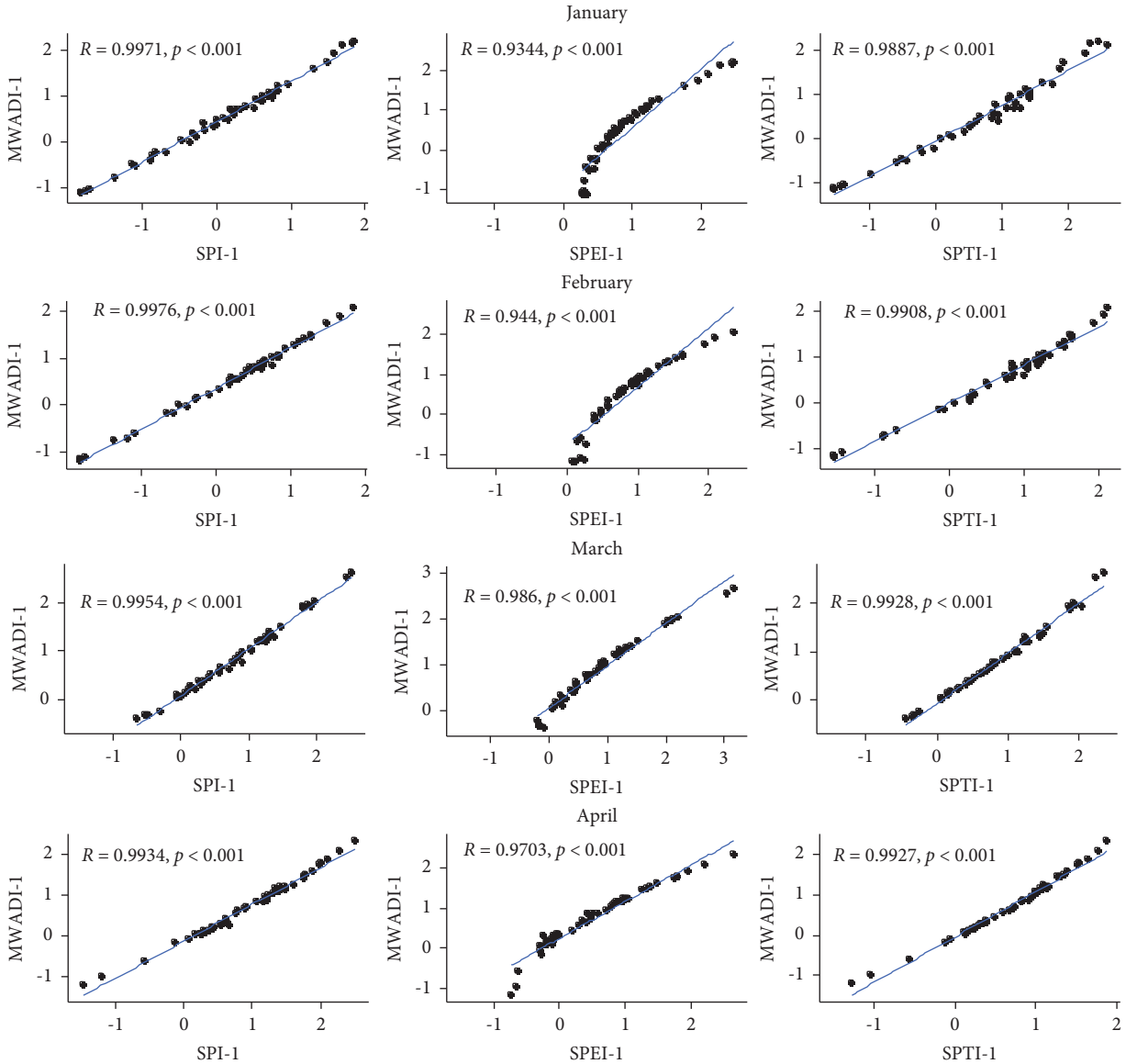

Figure 4: The scatter diagram and correlation coefficient R values between the seasonal MWADI and the SPI, the SPEI, and the SPTI (January–April) at Astore.

related to drought characterization. Furthermore, inaccurate drought characterization may mislead to drought mitigation policymakers. As the MWADI synthesized the climatic and meteorological characteristics of different SDIs (the SPI, the SPEI, and the SPTI), the drought characterization through the MWADI is considered more reliable. It reduces the uncertainty of drought characterization through different drought indices. The near normal (NN) drought class has a significantly higher proportion than other extreme classes. Extreme dry and extreme wet classes have comparatively lower count proportions but still can be catastrophic for linked ecosystems.

The temporal behavior of the MWADI and other SDIs (the SPI, the SPEI, and the SPTI) for the Astore station is shown in Figure 9. The SPI, the SPEI, and the SPTI were used to characterize short and long-term drought conditions. The graphical representation shows the evolution and termination of dry and wet conditions during 1970–2016. The red spikes and patches show the severity and duration of drought similarly; some blue spikes represent a few high precipitation events producing wet spells that cause flash flood events. The MWADI, the SPI, and the SPTI showed similar drought trends from 1970 to 2016, indicating the high correlation among these indices. This graphical evidence also clarifies the variation in defining drought classifications by the MWADI and other SDIs. The temporal behavior of the MWADI for a one-month time scale at all selected meteorological stations is presented in Figure 10. These statistical and graphical results indicate that the main advantage of the MWADI is its probabilistic graphical feature for characterizing and analyzing drought conditions. As the probabilistic structure of BNs is based on the cause-and-effect relationship between climatic and meteorological indicators therefore, a comprehensive drought index

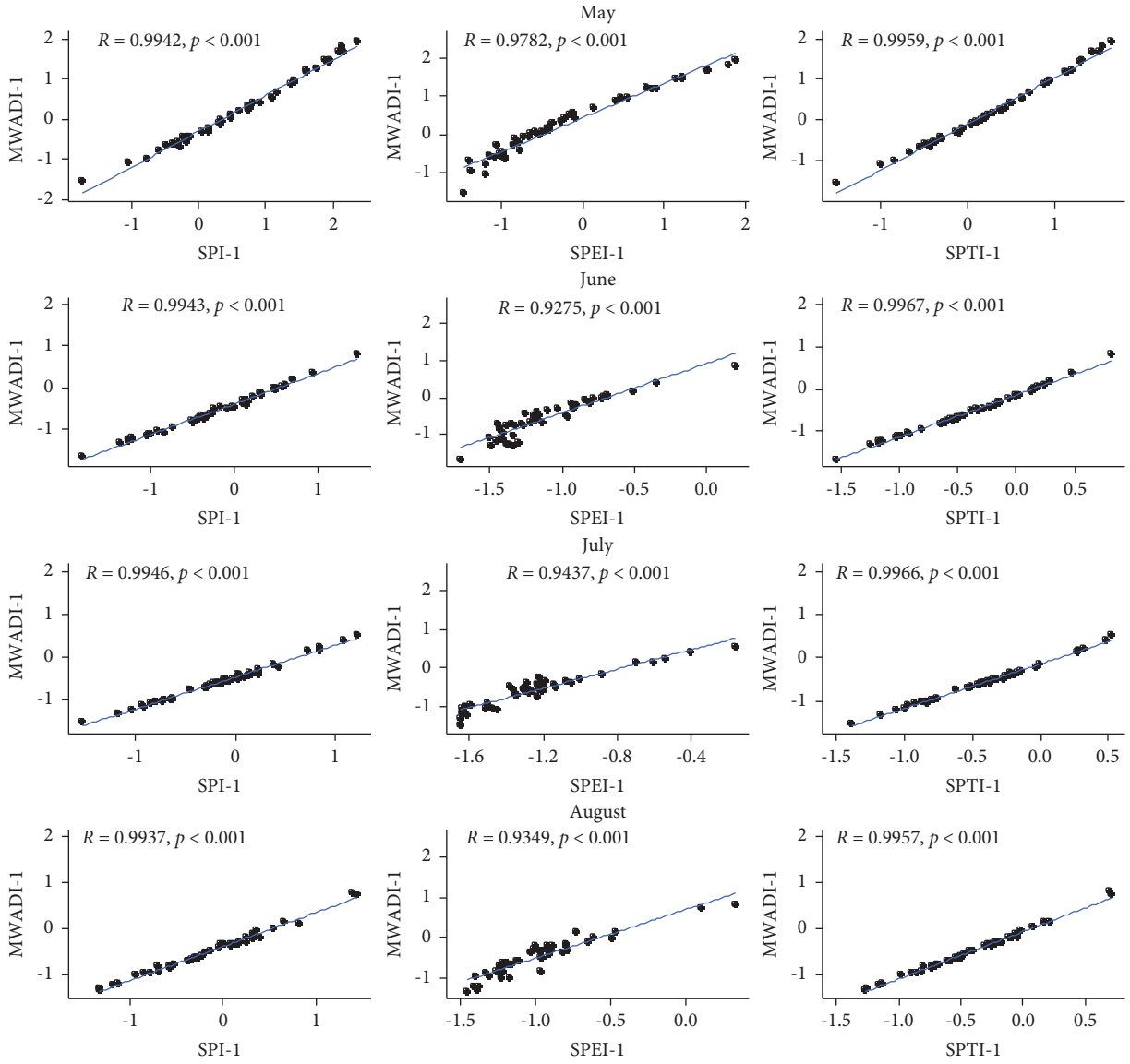

Figure 5: The scatter diagram and correlation coefficient R values between the seasonal MWADI and the SPI, the SPEI, and the SPTI (May–August) at Astore.

calculated through probabilistic structural and graphical algorithms reduces the uncertainties. The newly developed MWADI comprises various characteristics inherited by its multiple input multiscalar meteorological indicators. The MWADI can be easily implemented to display drought conditions across higher-order time scales. The temporal behavior of the MWADI at 6-month and 12-month time scales is presented in Figures 11 and 12 simultaneously. However, the proposed MWADI could be easily generalized by using more hydroclimatic and agricultural indicators as input variables for hydrological and agricultural drought assessment. Drought is a recurring threat to linked ecosystems, creating issues related to freshwater resources. The Bayesian network-based MWADI seems more promising for drought characterization to cope with such kinds of challenges.

The current study uses the SPI, the SPEI, and the SPTI as input indicators. These meteorological indicators are based on precipitation and mean monthly temperature, which defines the limits of the MWADI. The scope of the proposed index can be enhanced by using more input indicators based on soil moisture and remote sensing data. Similarly, different

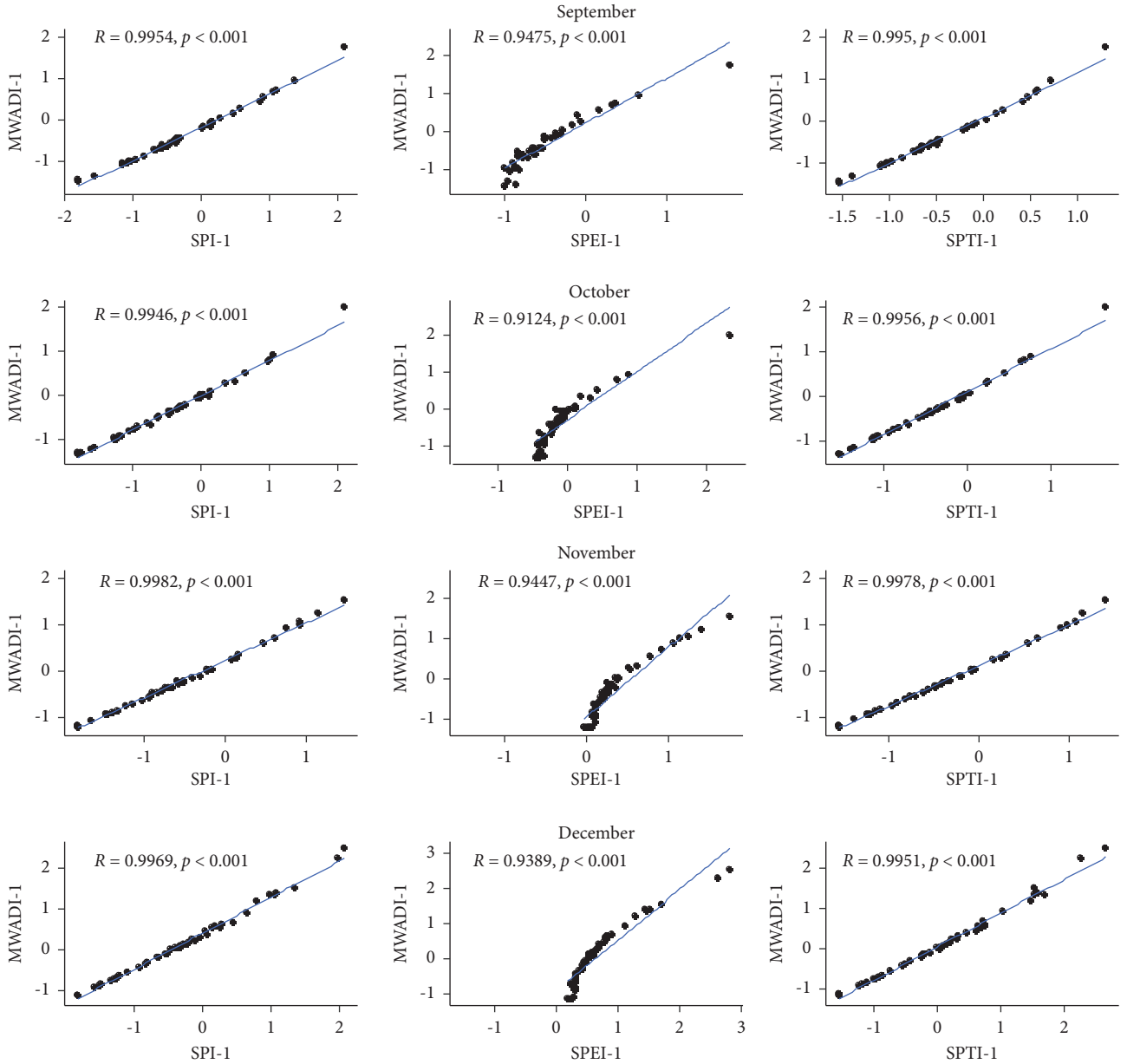

Figure 6: The scatter diagram and correlation coefficient R values between the seasonal MWADI and the SPI, the SPEI, and the SPTI (September–December) at Astore.

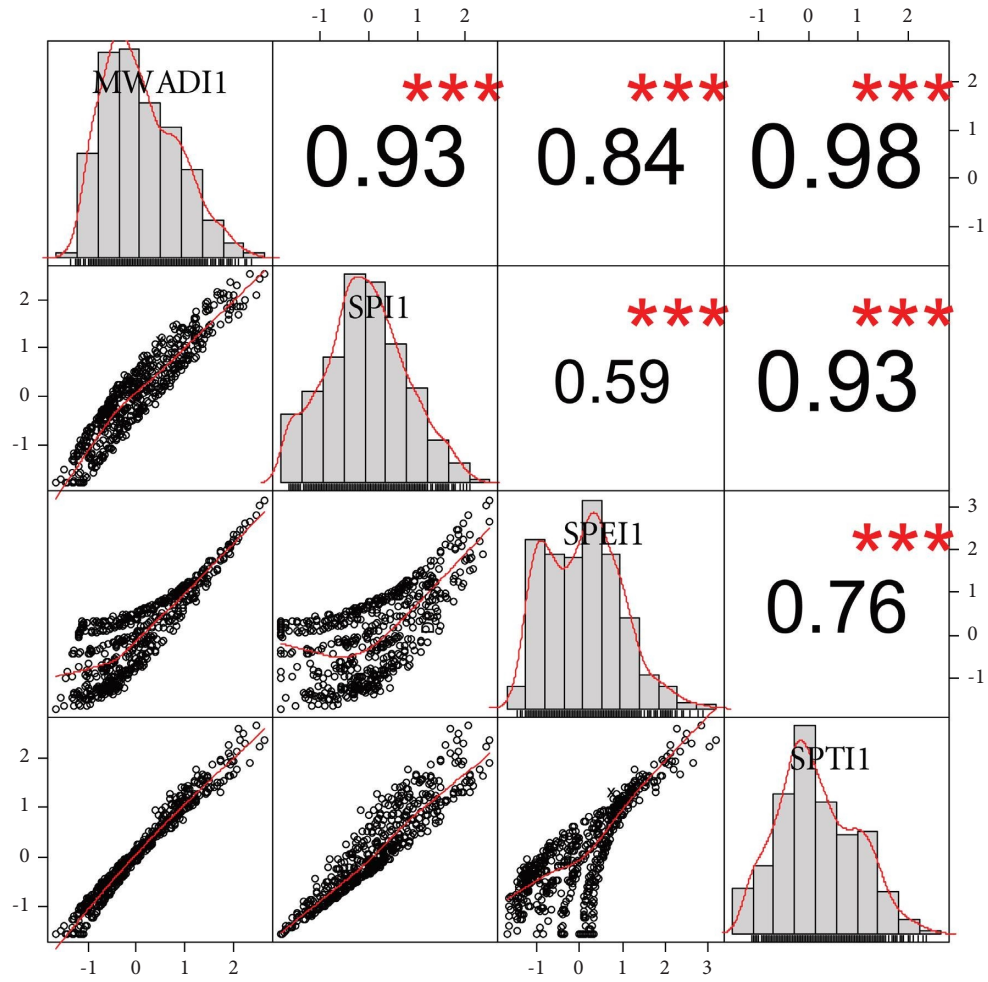

Figure 7: The correlation chart of the MWADI with other SDIs (the SPI, the SPEI, and the SPTI) at the Astore station.

Table 5: The correlation coefficient (r) for $MWADI_i$ with $SPI_i, SPEI_i$ and $SPTI_i$ at all meteorological stations for all seasons ($i = 1, 2, \cdots, 12$).

Seasons		Astore			Bunji			Chilas			Gilgit			Gupis			Skardu		
		SPI	SPEI	SPTI	SPI	SPEI	SPTI	SPI	SPEI	SPTI	SPI	SPEI	SPTI	SPI	SPEI	SPTI	SPI	SPEI	SPTI
Jan	MWADI	0.9971	0.9344	0.9887	0.9986	0.8824	0.9976	0.9986	0.8824	0.9976	0.9985	0.8329	0.9973	0.9984	0.9065	0.9976	0.9790	0.9236	0.9512
Feb		0.9976	0.9440	0.9908	0.9951	0.7957	0.9917	0.9951	0.7957	0.9916	0.9982	0.8384	0.9977	0.9940	0.7116	0.9967	0.9849	0.9383	0.9935
Mar		0.9954	0.9860	0.9928	0.9950	0.8875	0.9967	0.9950	0.8875	0.9967	0.9960	0.8571	0.9963	0.9958	0.8809	0.9968	0.9899	0.9590	0.9967
Apr		0.9934	0.9703	0.9927	0.9958	0.9276	0.9971	0.9958	0.9276	0.9971	0.9946	0.8806	0.9952	0.9951	0.8499	0.9937	0.9883	0.9565	0.9969
May		0.9942	0.9782	0.9959	0.9921	0.9202	0.9961	0.9921	0.9202	0.9961	0.9947	0.9107	0.9974	0.9911	0.9061	0.9947	0.9850	0.9596	0.9971
Jun		0.9943	0.9275	0.9967	0.9948	0.7784	0.9976	0.9948	0.7784	0.9976	0.9960	0.7629	0.9978	0.9937	0.8540	0.9954	0.9827	0.8107	0.9840
Jul		0.9946	0.9437	0.9966	0.9935	0.8725	0.9970	0.9935	0.8725	0.9970	0.9942	0.8262	0.9966	0.9927	0.7865	0.9951	0.9802	0.8382	0.9839
Aug		0.9937	0.9349	0.9957	0.9919	0.9055	0.9959	0.9919	0.9056	0.9959	0.9956	0.9070	0.9973	0.9939	0.8933	0.9950	0.9785	0.9027	0.9893
Sep		0.9954	0.9475	0.9950	0.9958	0.9022	0.9975	0.9958	0.9022	0.9975	0.9974	0.8699	0.9980	0.9935	0.8608	0.9945	0.9827	0.9391	0.9922
Oct		0.9946	0.9124	0.9956	0.9992	0.8855	0.9989	0.9992	0.8855	0.9989	0.9935	0.7857	0.9921	0.9944	0.8069	0.9939	0.9761	0.9112	0.9936
Nov		0.9982	0.9447	0.9978	0.9992	0.9005	0.9984	0.9992	0.9005	0.9984	0.9993	0.9029	0.9990	0.9987	0.8589	0.9986	0.9911	0.9607	0.9962
Dec		0.9969	0.9389	0.9951	0.9987	0.8538	0.9961	0.9987	0.8538	0.9961	0.9993	0.8889	0.9977	0.9986	0.8349	0.9964	0.9914	0.9456	0.9978

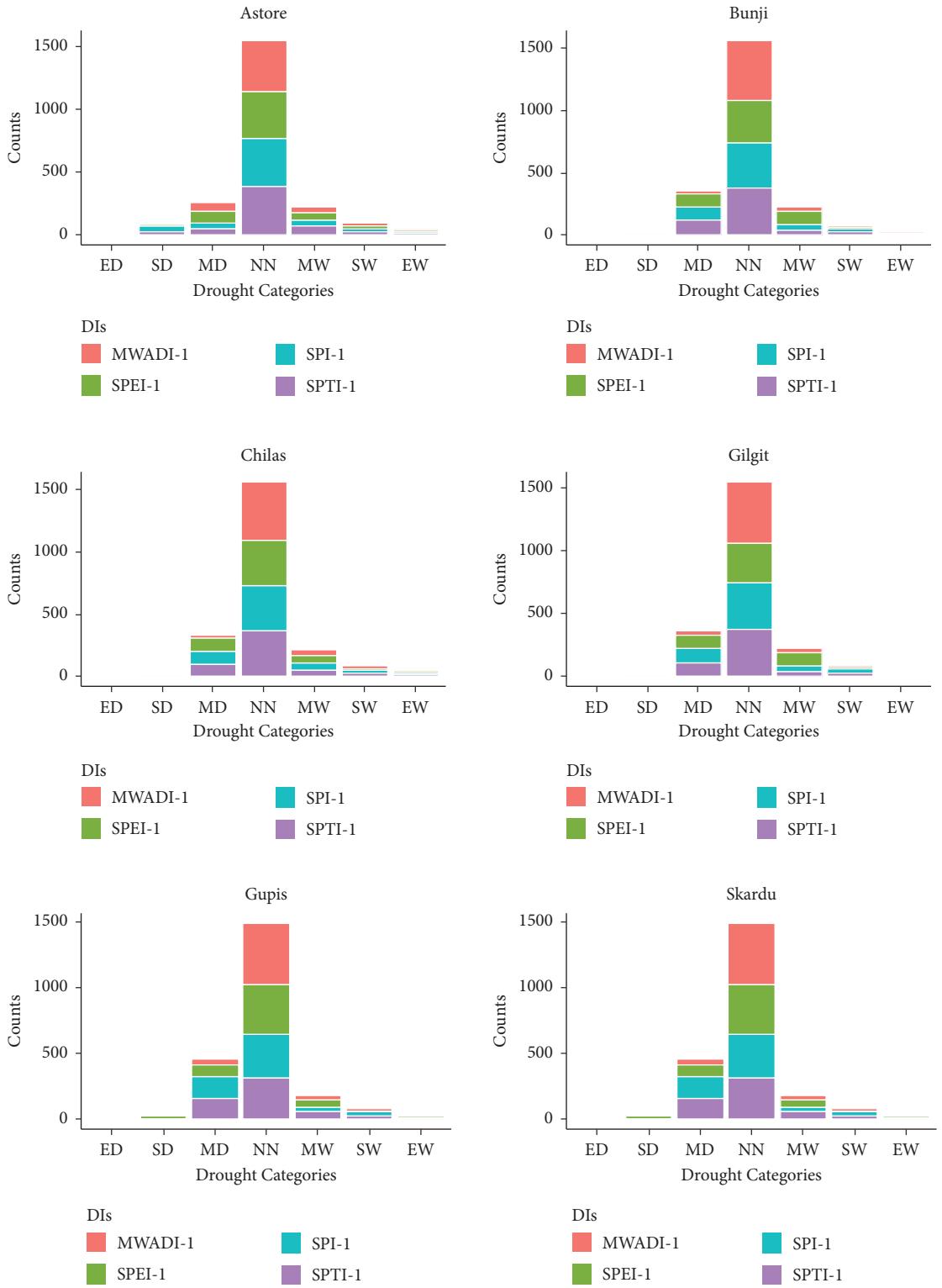

Figure 8: Count plots of MWADI-1, SPI-1, SPEI-1, and SPTI-1 at all stations.

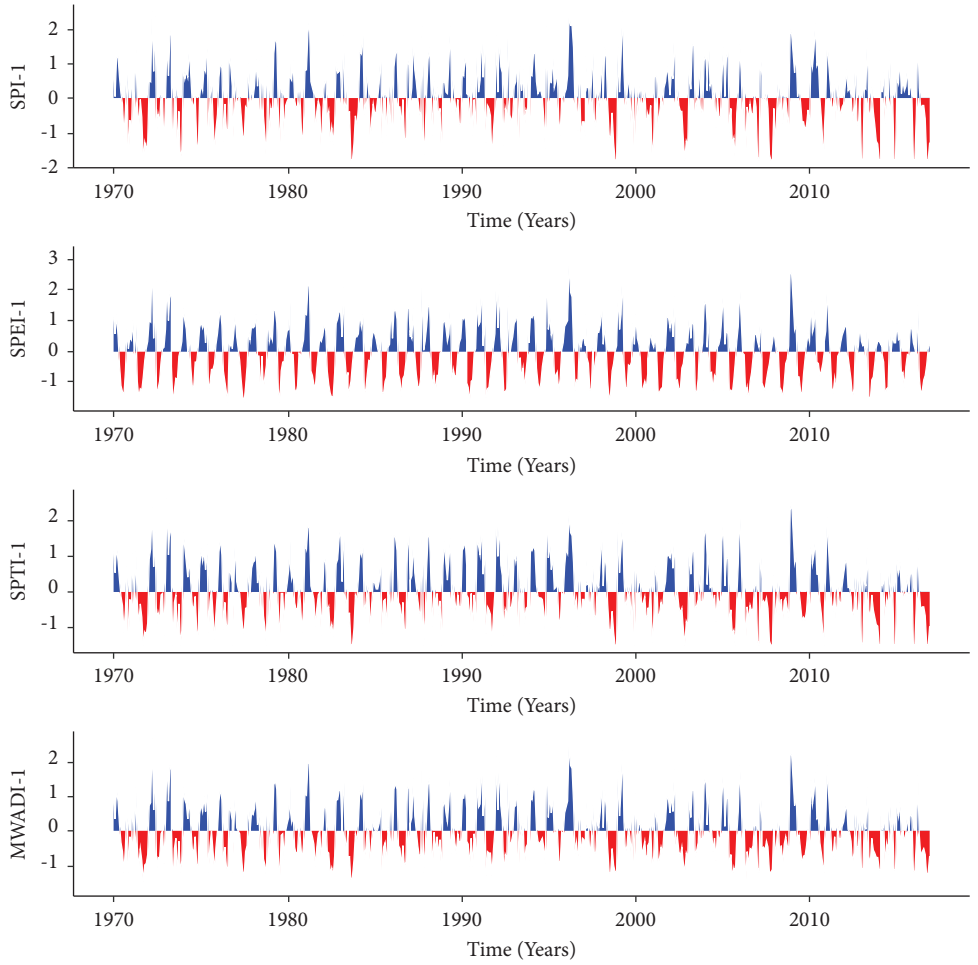

Figure 9: Temporal plots comparison of MWADI-1 with SPI-1, SPEI-1, and SPTI-1 at the Astore station.

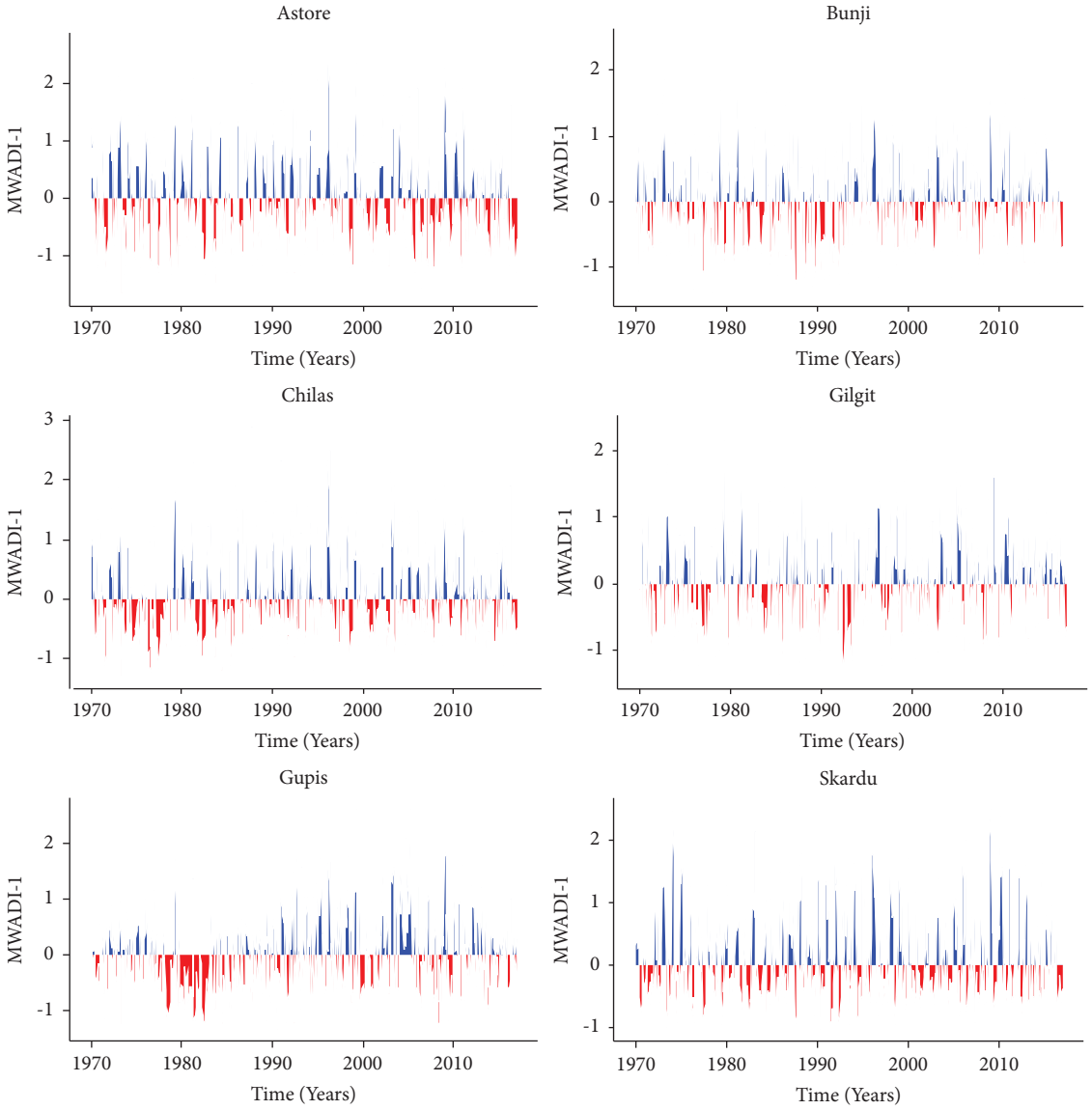

Figure 10: Temporal behavior of the MWADI at one-month time scale at all stations.

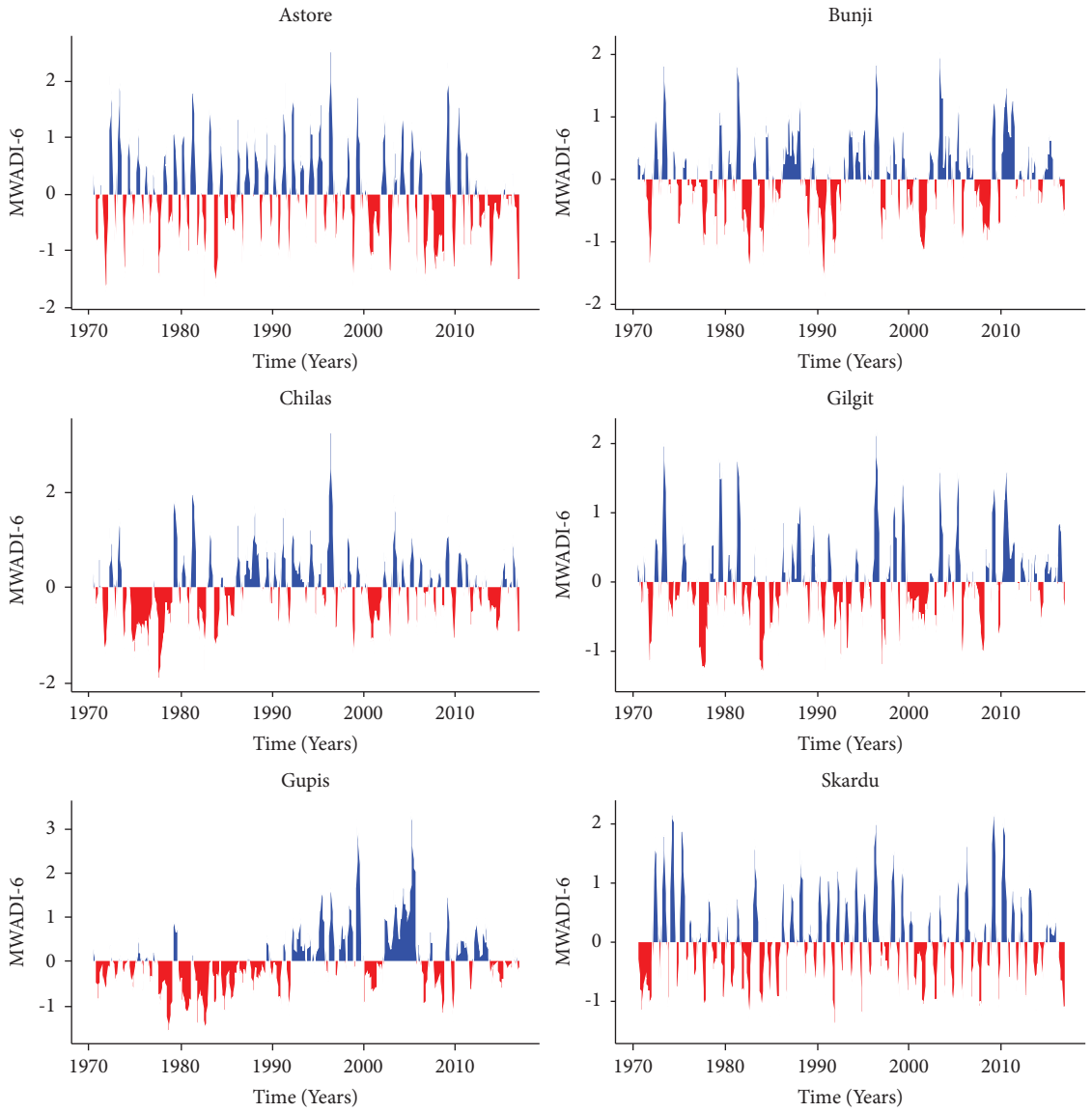

Figure 11: Temporal behavior of the MWADI at 6-month time scale at all stations.

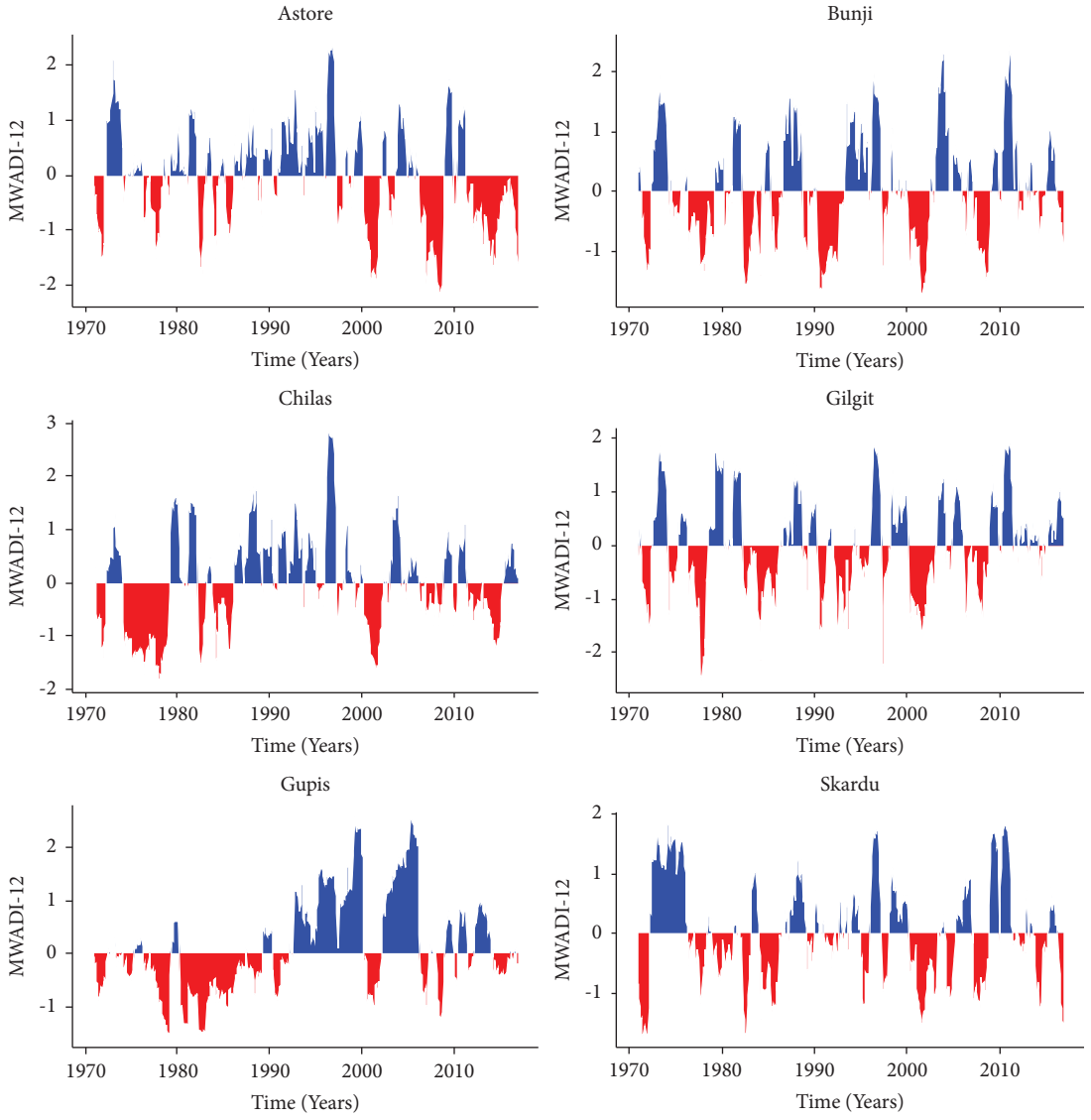

Figure 12: Temporal behavior of the MWADI at 12-month time scale at all stations.

drought indices could be combined using alternative stochastic and multivariate algorithms such as copulas and principal component analysis (PCA), which can be considered as future directions.

4. Conclusion

The use of a single drought index provides insufficient information related to the drought assessment. Due to the complex nature and widespread impacts of drought, applying a single index creates uncertainty for drought assessment and monitoring. Therefore, a new comprehensive procedure is required to minimize the uncertainty of drought evaluation. In this regard, the current study proposes a new framework, known as the multiscalar weighted amalgamated drought index (MWADI), that synthesizes information from multiple drought indices. The MWADI is mainly based on the ADPPs. Furthermore, these ADPPs are based on Bayesian networks (BNs)-based Monte Carlo Markov Chain (MCMC) simulations. The MWADI reconciles different drought indices and helps decision-makers to understand drought-related uncertainties. The drought severity and episodes estimated by the MWADI are compared and verified by temporal plots, count plots, and correlation charts. Moreover, the results of the MWADI are compared with the SPI, the SPEI, and the SPTI to estimate the drought events (impacts). The associated outcomes of the MWADI show a positive relationship with the SPI and the SPTI. Therefore, the MWADI can capture small changes in drought patterns and comprehensive drought risk assessment at the selected climatic zone.

Data Availability

The secondary data used to validate the proposed methods are available from the corresponding authors upon request.

Conflicts of Interest

The authors declare that they have no conflicts of interest.

Acknowledgments

Their authors extend their appreciation to the Deanship of Scientific Research at King Khalid University for funding this work through large groups Research project under grant number (RGP.2/23/44). And this study was supported via funding from Prince Sattam bin Abdulaziz University (project number (PSAU/2023/R/1444)).

References

[1] M. Agnoletti, A. Errico, A. Santoro, A. Dani, and F. Preti, "Terraced landscapes and hydrogeological risk. Effects of land abandonment in Cinque Terre (Italy) during severe rainfall events," *Sustainability*, vol. 11, no. 1, p. 235, 2019.

[2] A. AghaKouchak, A. Farahmand, F. S. Melton et al., "Remote sensing of drought: progress, challenges, and opportunities," *Reviews of Geophysics*, vol. 53, no. 2, pp. 452–480, 2015.

[3] D. A. Wilhite and M. H. Glantz, "Understanding: the drought phenomenon: the role of definitions," *Water International*, vol. 10, no. 3, pp. 111–120, 1985.

[4] R. R. Heim Jr, "A review of twentieth-century drought indices used in the United States," *Bulletin of the American Meteorological Society*, vol. 83, no. 8, pp. 1149–1166, 2002.

[5] A. Kaur and S. K. Sood, "Artificial intelligence-based model for drought prediction and forecasting," *The Computer Journal*, vol. 63, no. 11, pp. 1704–1712, 2020.

[6] N. Wanders and Y. Wada, "Human and climate impacts on the 21st century hydrological drought," *Journal of Hydrology*, vol. 526, pp. 208–220, 2015.

[7] S. H. Pour, A. K. A. Wahab, and S. Shahid, "Physical-empirical models for prediction of seasonal rainfall extremes of Peninsular Malaysia," *Atmospheric Research*, vol. 233, Article ID 104720, 2020.

[8] U. Büntgen, O. Urban, P. J. Krusic et al., "Recent European drought extremes beyond Common Era background variability," *Nature Geoscience*, vol. 14, no. 4, pp. 190–196, 2021.

[9] A. K. Mishra and V. P. Singh, "A review of drought concepts," *Journal of Hydrology*, vol. 391, no. 1-2, pp. 202–216, 2010.

[10] S. Mohamadi, S. S. Sammen, F. Panahi et al., "Zoning map for drought prediction using integrated machine learning models with a nomadic people optimization algorithm," *Natural Hazards*, vol. 104, no. 1, pp. 537–579, 2020.

[11] L. Gu, J. Chen, J. Yin et al., "Projected increases in magnitude and socioeconomic exposure of global droughts in 1.5 and 2 C warmer climates," *Hydrology and Earth System Sciences*, vol. 24, no. 1, pp. 451–472, 2020.

[12] P. Wang, W. Qiao, Y. Wang, S. Cao, and Y. Zhang, "Urban drought vulnerability assessment–A framework to integrate socioeconomic, physical, and policy index in a vulnerability contribution analysis," *Sustainable Cities and Society*, vol. 54, Article ID 102004, 2020.

[13] E. Gidey, O. Dikinya, R. Sebego, E. Segosebe, and A. Zenebe, "Analysis of the long-term agricultural drought onset, cessation, duration, frequency, severity and spatial extent using Vegetation Health Index (VHI) in Raya and its environs, Northern Ethiopia," *Environmental Systems Research*, vol. 7, no. 1, pp. 13–18, 2018.

[14] M. D. Svoboda and B. A. Fuchs, *Handbook of Drought Indicators and Indices*, World Meteorological Organization, Geneva, Switzerland, 2016.

[15] S. R. Chikabvumbwa, N. Salehnia, R. Manzanas, C. Abdelbaki, and A. Zerga, "Assessing the effect of spatial–temporal droughts on dominant crop yield changes in Central Malawi," *Environmental Monitoring and Assessment*, vol. 194, no. 2, pp. 63–16, 2022.

[16] A. Malik, Y. Tikhamarine, S. S. Sammen, S. I. Abba, and S. Shahid, "Prediction of meteorological drought by using hybrid support vector regression optimized with HHO versus PSO algorithms," *Environmental Science & Pollution Research*, vol. 28, no. 29, pp. 39139–39158, 2021.

[17] W. C. Palmer, *Meteorological Drought*, US Weather Bureau, Washington, DC, USA, 1965.

[18] B. A. Shafer and L. E. Dezman, "Development of surface water supply index (SWSI) to assess the severity of drought condition in snowpack runoff areas," in *Proceedings of the Western Snow Conference*, Reno, Nevada, January, 1982.

[19] T. B. McKee, N. J. Doesken, and J. Kleist, "The relationship of drought frequency and duration to time scales," in *Proceedings of the 8th Conference on Applied Climatology*, vol. 17, no. 22, pp. 179–183, American Meteorological Society, Boston, MA, USA, January, 1993.

[20] H. R. Byun and D. A. Wilhite, "Objective quantification of drought severity and duration," *Journal of Climate*, vol. 12, no. 9, pp. 2747–2756, 1999.

[21] S. M. Vicente-Serrano, S. Beguería, and J. I. López-Moreno, "A multiscalar drought index sensitive to global warming: the standardized precipitation evapotranspiration index," *Journal of Climate*, vol. 23, no. 7, pp. 1696–1718, 2010.

[22] Z. Ali, I. Hussain, M. Faisal et al., "A novel multiscalar drought index for monitoring drought: the standardized precipitation temperature index," *Water Resources Management*, vol. 31, no. 15, pp. 4957–4969, 2017.

[23] H. R. Byun and D. W. Kim, "Comparing the effective drought index and the standardized precipitation index," *Economics of drought and drought preparedness in a climate change context. López-Francos A.(comp.), López-Francos A.(collab.). Options Méditerranéennes. Sér. A. Séminaires Méditerranéens*, vol. 95, pp. 85–89, 2010.

[24] S. Kim, P. Parhi, H. Jun, and J. Lee, "Evaluation of drought severity with a Bayesian network analysis of multiple drought indices," *Journal of Water Resources Planning and Management*, vol. 144, no. 1, Article ID 05017016, 2018.

[25] M. Waseem, M. Ajmal, and T. W. Kim, "Development of a new composite drought index for multivariate drought assessment," *Journal of Hydrology*, vol. 527, pp. 30–37, 2015.

[26] L. Gu, J. Chen, J. Yin, C. Y. Xu, and H. Chen, "Drought hazard transferability from meteorological to hydrological propagation," *Journal of Hydrology*, vol. 585, Article ID 124761, 2020.

[27] T. Ji, G. Li, H. Yang, R. Liu, and T. He, "Comprehensive drought index as an indicator for use in drought monitoring integrating multi-source remote sensing data: a case study covering the Sichuan-Chongqing region," *International Journal of Remote Sensing*, vol. 39, no. 3, pp. 786–809, 2018.

[28] G. Qaiser, S. Tariq, S. Adnan, and M. Latif, "Evaluation of a composite drought index to identify seasonal drought and its associated atmospheric dynamics in Northern Punjab, Pakistan," *Journal of Arid Environments*, vol. 185, Article ID 104332, 2021.

[29] J. F. Brown, B. D. Wardlow, T. Tadesse, M. J. Hayes, and B. C. Reed, "The Vegetation Drought Response Index (VegDRI): a new integrated approach for monitoring drought stress in vegetation," *GIScience and Remote Sensing*, vol. 45, no. 1, pp. 16–46, 2008.

[30] K. C. Mo and D. P. Lettenmaier, "Objective drought classification using multiple land surface models," *Journal of Hydrometeorology*, vol. 15, no. 3, pp. 990–1010, 2014.

[31] H. Han, J. Bai, J. Yan, H. Yang, and G. Ma, "A combined drought monitoring index based on multi-sensor remote sensing data and machine learning," *Geocarto International*, vol. 36, no. 10, pp. 1161–1177, 2021.

[32] D. Heckerman, "Learning in graphical models, chapter A tutorial on learning with bayesian networks," *Adaptive Computation and Machine Learning*, pp. 301–354, MIT Press, Cambridge, MA, USA, 1999.

[33] P. Johnson, M. Ekstedt, and R. Lagerstrom, "Automatic probabilistic enterprise IT architecture modeling: a dynamic bayesian networks approach," in *Proceedings of the 2016 IEEE 20th International Enterprise Distributed Object Computing Workshop (EDOCW)*, pp. 1–8, IEEE, Vienna, Austria, September, 2016.

[34] L. Duan and Y. Xiong, "Big data analytics and business analytics," *Journal of Management Analytics*, vol. 2, no. 1, pp. 1–21, 2015.

[35] E. Pérez-Miñana, P. J. Krause, and J. Thornton, "Bayesian Networks for the management of greenhouse gas emissions in the British agricultural sector," *Environmental Modelling & Software*, vol. 35, pp. 132–148, 2012.

[36] M. Scutari, P. Howell, D. J. Balding, and I. Mackay, "Multiple quantitative trait analysis using Bayesian networks," *Genetics*, vol. 198, no. 1, pp. 129–137, 2014.

[37] L. Kaikkonen, T. Parviainen, M. Rahikainen, L. Uusitalo, and A. Lehikoinen, "Bayesian networks in environmental risk assessment: a review," *Integrated Environmental Assessment and Management*, vol. 17, no. 1, pp. 62–78, 2021.

[38] P. A. Aguilera, A. Fernández, R. Fernández, R. Rumí, and A. Salmerón, "Bayesian networks in environmental modelling," *Environmental Modelling & Software*, vol. 26, no. 12, pp. 1376–1388, 2011.

[39] A. Sperotto, J. L. Molina, S. Torresan, A. Critto, M. Pulido-Velazquez, and A. Marcomini, "A Bayesian Networks approach for the assessment of climate change impacts on nutrients loading," *Environmental Science & Policy*, vol. 100, pp. 21–36, 2019.

[40] Y. Wu, W. Xu, J. Feng, S. Palaiahnakote, and T. Lu, "Local and global Bayesian network based model for flood prediction," in *Proceedings of the 2018 24th International Conference on Pattern Recognition (ICPR)*, pp. 225–230, IEEE, Beijing, China, August, 2018.

[41] C. Vitolo, M. Scutari, M. Ghalaieny, A. Tucker, and A. Russell, "Modeling air pollution, climate, and health data using Bayesian Networks: a case study of the English regions," *Earth and Space Science*, vol. 5, no. 4, pp. 76–88, 2018.

[42] R. Ávila and D. Ballari, "A bayesian network approach to identity climate teleconnections within homogeneous precipitation regions in Ecuador," in *Proceedings of the Conference on Information Technologies and Communication of Ecuador*, pp. 21–35, Springer, Cham, Switzerland, November, 2019.

[43] S. C. Kao and R. S. Govindaraju, "A copula-based joint deficit index for droughts," *Journal of Hydrology*, vol. 380, no. 1-2, pp. 121–134, 2010.

[44] S. Chen, W. Zhong, S. Pan, Q. Xie, and T. W. Kim, "Comprehensive drought assessment using a modified composite drought index: a case study in Hubei Province, China," *Water*, vol. 12, no. 2, p. 462, 2020.

[45] D. Cui, W. Yuan, C. Chen, and R. Han, "Identification of colorectal cancer-associated macrophage biomarkers by integrated bioinformatic analysis," *International Journal of Clinical and Experimental Pathology*, vol. 14, pp. 1–8, 2021.

[46] W. Köppen, "Die Wärmezonen der Erde, nach der Dauer der heissen, gemässigten und kalten Zeit und nach der Wirkung der Wärme auf die organische Welt betrachtet," *Meteorologische Zeitschrift*, vol. 1, no. 21, pp. 5–226, 1884.

[47] J. Sheffield, E. F. Wood, N. Chaney et al., "A drought monitoring and forecasting system for sub-Sahara African water resources and food security," *Bulletin of the American Meteorological Society*, vol. 95, no. 6, pp. 861–882, 2014.

[48] N. B. Guttman, "Accepting the standardized precipitation index: a calculation algorithm 1," *JAWRA Journal of the American Water Resources Association*, vol. 35, no. 2, pp. 311–322, 1999.

[49] A. K. Mishra and V. R. Desai, "Drought forecasting using stochastic models," *Stochastic Environmental Research and Risk Assessment*, vol. 19, no. 5, pp. 326–339, 2005.

[50] J. H. Stagge, L. M. Tallaksen, L. Gudmundsson, A. F. Van Loon, and K. Stahl, "Candidate distributions for

climatological drought indices (SPI and SPEI)," *International Journal of Climatology*, vol. 35, no. 13, pp. 4027–4040, 2015.
[51] Z. Hao, V. P. Singh, and Y. Xia, "Seasonal drought prediction: advances, challenges, and future prospects," *Reviews of Geophysics*, vol. 56, no. 1, pp. 108–141, 2018.
[52] E. Dutra, L. Magnusson, F. Wetterhall et al., "The 2010–2011 drought in the Horn of Africa in ECMWF reanalysis and seasonal forecast products," *International Journal of Climatology*, vol. 33, no. 7, pp. 1720–1729, 2013.
[53] K. C. Mo and B. Lyon, "Global meteorological drought prediction using the North American multi-model ensemble," *Journal of Hydrometeorology*, vol. 16, no. 3, pp. 1409–1424, 2015.
[54] J. H. Yoon, K. Mo, and E. F. Wood, "Dynamic-model-based seasonal prediction of meteorological drought over the contiguous United States," *Journal of Hydrometeorology*, vol. 13, no. 2, pp. 463–482, 2012.
[55] B. O. Ayugi, W. Wen, and D. Chepkemoi, "Analysis of spatial and temporal patterns of rainfall variations over Kenya," *Studies*, vol. 6, no. 11, 2016.
[56] Y. G. Yang, J. F. Hu, H. L. Xiao, S. B. Zou, and Z. L. Yin, "Spatial and temporal variations of hydrological characteristic on the landscape zone scale in alpine cold region," *Huan jing ke xue= Huanjing kexue*, vol. 34, no. 10, pp. 3797–3803, 2013.
[57] J. Pearl, "Bayesian networks: a model cf self-activated memory for evidential reasoning," in *Proceedings of the 7th conference of the Cognitive Science Society*, pp. 15–17, University of California, Irvine, CA, USA, August, 1985.
[58] J. Pearl, *Probabilistic Reasoning in Intelligent Systems: Networks of Plausible Inference*, Elsevier, Amsterdam, Netherlands, 2014.
[59] N. Friedman and D. Koller, "Being Bayesian about network structure. A Bayesian approach to structure discovery in Bayesian networks," *Machine Learning*, vol. 50, no. 1, pp. 95–125, 2003.
[60] S. Dey and J. A. Stori, "A Bayesian network approach to root cause diagnosis of process variations," *International Journal of Machine Tools and Manufacture*, vol. 45, no. 1, pp. 75–91, 2005.
[61] I. Ben-Gal, *Encyclopedia of Statistics in Quality and Reliability*John Wiley & Sons, Hoboken, NJ, USA, 2007.
[62] D. Madigan, J. York, and D. Allard, "Bayesian graphical models for discrete data," *International Statistical Review/ Revue Internationale de Statistique*, vol. 63, no. 2, pp. 215–232, 1995.
[63] D. Madigan, A. E. Raftery, C. Volinsky, and J. Hoeting, "Bayesian model averaging," in *Proceedings of the AAAI Workshop on Integrating Multiple Learned Models*, pp. 77–83, Portland, OR, USA, August, 1996.
[64] P. Giudici and R. Castelo, "Improving Markov chain Monte Carlo model search for data mining," *Machine Learning*, vol. 50, no. 1/2, pp. 127–158, 2003.
[65] M. Grzegorczyk and D. Husmeier, "Improving the structure MCMC sampler for Bayesian networks by introducing a new edge reversal move," *Machine Learning*, vol. 71, no. 2-3, pp. 265–305, 2008.
[66] A. Raza, I. Hussain, Z. Ali et al., "A seasonally blended and regionally integrated drought index using Bayesian network theory," *Meteorological Applications*, vol. 28, no. 3, 2021.
[67] S. Madadgar and H. Moradkhani, "A Bayesian framework for probabilistic seasonal drought forecasting," *Journal of Hydrometeorology*, vol. 14, no. 6, pp. 1685–1705, 2013.
[68] M. Kavianpour, M. Seyedabadi, and S. Moazami, "Spatial and temporal analysis of drought based on a combined index using copula," *Environmental Earth Sciences*, vol. 77, no. 22, pp. 769–812, 2018.
[69] J. Won, J. Choi, O. Lee, and S. Kim, "Copula-based Joint Drought Index using SPI and EDDI and its application to climate change," *Science of the Total Environment*, vol. 744, Article ID 140701, 2020.
[70] Y. Li, Y. Gong, and C. Huang, "Construction of combined drought index based on bivariate joint distribution," *Alexandria Engineering Journal*, vol. 60, no. 3, pp. 2825–2833, 2021.
[71] J. Y. Shin, H. H. Kwon, J. H. Lee, and T. W. Kim, "Probabilistic long-term hydrological drought forecast using Bayesian networks and drought propagation," *Meteorological Applications*, vol. 27, no. 1, 2020.
[72] B. Zhang, X. Zhao, J. Jin, and P. Wu, "Development and evaluation of a physically based multiscalar drought index: the Standardized Moisture Anomaly Index," *Journal of Geophysical Research: Atmospheres*, vol. 120, no. 22, pp. 11,575–11,588, 2015.
[73] X. Li, B. He, X. Quan, Z. Liao, and X. Bai, "Use of the standardized precipitation evapotranspiration index (SPEI) to characterize the drying trend in southwest China from 1982–2012," *Remote Sensing*, vol. 7, no. 8, pp. 10917–10937, 2015.